Squark contributions to photon structure functions and positivity constraints

Yoshio Kitadono[*] and Yutaka Yoshida[†]

High Energy Accelerator Research Organization (KEK), 1-1 Oh-ho, Tsukuba, Ibaraki 305-0801, Japan

Ryo Sahara[‡] and Tsuneo Uematsu[§]

Department of Physics, Graduate School of Science, Kyoto University, Kitashirakawa, Kyoto 606-8502, Japan

Photon structure functions in supersymmetric QCD are investigated in terms of the parton model where squark contributions are evaluated. We calculate the eight virtual photon structure functions by taking the discontinuity of the squark massive one-loop diagrams of the photon-photon forward amplitude. The model-independent positivity constraints derived from the Cauchy-Schwarz inequalities are satisfied by the squark parton model calculation and actually the two equality relations hold for the squark contribution. We also show that our polarized photon structure function g_1^γ for the real photon leads to the vanishing first moment sum rule, and the constraint $|g_1^\gamma| \le F_1^\gamma$ is satisfied by the real photon. We also discuss a squark signature in the structure function W_{TT}^τ.

I. INTRODUCTION

The Large Hadron Collider (LHC) [1] has restarted its operation and it is anticipated that the signals for the Higgs boson as well as the new physics beyond standard model, such as an evidence for the supersymmetry (SUSY), might be discovered. Once these signals are observed more precise measurement needs to be carried out at the future e^+e^- collider, so called International Linear Collider (ILC) [2].

It is well known that, in e^+e^- collision experiments, the cross section for the two-photon processes $e^+e^- \to e^+e^- +$ hadrons dominates at high energies over the one-photon annihilation process $e^+e^- \to \gamma^* \to$ hadrons. We consider here the two-photon processes in the double-tag events where both of the outgoing e^+ and e^- are detected. Especially, the case in which one of the virtual photons is far off shell (large $Q^2 \equiv -q^2$), while the other is close to the mass shell (small $P^2 = -p^2$), can be viewed as a deep-inelastic scattering where the target is a photon rather than a nucleon [3]. In this deep-inelastic scattering off photon targets, we can study the photon structure functions [4], which are the analogues of the nucleon structure functions.

In order to analyze the two-photon process including new heavy particles at ILC, it is important to consider the mass effects of the new heavy particles, like supersymmetric particles. In this paper we investigate contribution from the squarks, the superpartner of the quarks, to the photon structure functions. Before the supersymmetric QCD

radiative effects are studied taking into account the mass effects, it is worthwhile, first, to investigate squark contributions to the photon structure functions through the pure QED interaction fully taking into account the squark mass effects. We evaluate the eight virtual photon structure functions by taking the discontinuity of the squark one-loop diagrams of the photon-photon forward amplitude. We study the model-independent positivity constraints whether squark parton model calculation satisfies these constraints. The real photon case is recovered by putting P^2 (target photon mass squared) equal to zero.

The real unpolarized photon structure functions, F_2^γ and F_L^γ, were investigated by the parton model (PM) in [5] and were studied by the operator product expansion (OPE) supplemented with the renormalization group equation method [6,7] and were calculated by improved PM powered by the evolution equations [8–11]. In the case that the mass squared of the target photon is nonvanishing ($P^2 \ne 0$), we can investigate the virtual photon structure functions. The unpolarized virtual photon structure functions were studied to LO in [12] and to next-to-leading order (NLO) in [13–16]. Parton contents were studied in [17,18] and the target mass effect of virtual photon structure functions in LO was discussed in [19]. The heavy-quark mass effects in photon structure functions were studied in the literature [9,18,20–27]. See, for example, the recent work by pQCD [28–31], by AdS/QCD [32], and references therein. The polarized photon structure function g_1^γ was investigated with pQCD up to the leading order (LO) [33,34], and the NLO [20,21,35,36].

The general forward photon-photon scattering amplitude is characterized by the helicity amplitudes and those are decomposed into eight tensor structures [37–40]. But we have four-independent structure functions in the case that the target photon is on shell. The results of four-independent real photon structure functions W_{TT}, W_{TT}^a,

---

[*]Current address: Institute of Physics, Academia Sinica, Taipei, Taiwan.
kitadono@phys.sinica.edu.tw
[†]yyoshida@post.kek.jp
[‡]sahara@scphys.kyoto-u.ac.jp
[§]uematsu@scphys.kyoto-u.ac.jp

W_{TT}^τ, W_{LT} by the quark parton model (QPM) to the leading order (LO) in QED were derived in Ref. [41] and the results of eight independent virtual photon structure functions by the QPM were obtained in Ref. [42] (also see Ref. [43]). In these references [41,42], the three positivity constraints were derived for the virtual photon target by using the Cauchy-Schwarz inequality and those reduce to one constraint in the real photon limit. All results satisfied with these constraints up to the leading order in QED.

On the other hand, the photon structure functions in supersymmetric theories were studied in Refs. [44–47] up to the leading order in SUSY QED. In these references, the real photon structure functions F_2^γ and F_L^γ were considered instead of the four-independent photon structure functions. Furthermore, the study of the polarized real photon g_1^γ will be important theoretically and phenomenologically, since the polarized photon structure function g_1^γ has a remarkable sum rule, $\int_0^1 g_1^\gamma(x, Q^2)dx = 0$ [48–52]. Another constraint $|g_1^\gamma| \leq F_1^\gamma$ is derived in Refs. [20,35]. We will show that our result for the polarized photon structure function satisfies this sum rule and the constraint between g_1^γ and F_1^γ.

In the next section, we discuss the general framework of eight virtual photon structure functions and positivity constraints. In Sec. III, we present our calculation of squark contributions to the photon structure functions and the numerical analysis is carried out. In Sec. IV, we examine various aspects of the real photon structure functions, like inequality between g_1^γ and F_1^γ and the vanishing first moment sum rule. In Sec. V, we discuss a possible signature for the squark in the structure function W_{TT}^τ. The final section is devoted to the conclusion.

II. PHOTON STRUCTURE FUNCTIONS AND POSITIVITY CONSTRAINTS

We consider the virtual photon-photon forward scattering amplitude for $\gamma(q) + \gamma(p) \rightarrow \gamma(q) + \gamma(p)$ illustrated in Fig. 1,

$$T_{\mu\nu\rho\sigma}(p, q) = i \int d^4x d^4y d^4z e^{iq\cdot x} e^{ip\cdot(y-z)}$$
$$\times \langle 0|T(J_\mu(x)J_\nu(0)J_\rho(y)J_\sigma(z))|0\rangle, \quad (2.1)$$

where J is the electromagnetic current, q and p are the four-momenta of the probe and target photon, respectively. The s-channel helicity amplitudes are related to its absorptive part as follows:

$$W(ab|a'b') = \epsilon_\mu^*(a)\epsilon_\rho^*(b)W^{\mu\nu\rho\sigma}\epsilon_\nu(a')\epsilon_\sigma(b'), \quad (2.2)$$

where

$$W_{\mu\nu\rho\sigma}(p, q) = \frac{1}{\pi} \operatorname{Im}T_{\mu\nu\rho\sigma}(p, q), \quad (2.3)$$

and $\epsilon_\mu(a)$ represents the photon polarization vector with helicity a, and $a = 0, \pm 1$. Similarly for the other
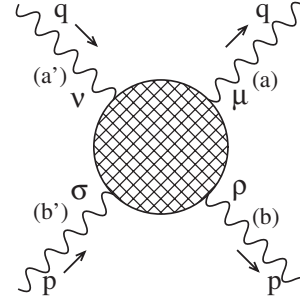

FIG. 1. Virtual photon-photon forward scattering with momenta $q(p)$ and helicities $a(b)$ and $a'(b')$.

polarization vectors and we have $a', b, b' = 0, \pm 1$. Because of the angular momentum conservation, parity conservation, and time reversal invariance [53], we have in total eight independent s-channel helicity amplitudes, which we may take as

$$W(1, 1|1, 1), \quad W(1, -1|1, -1), \quad W(1, 0|1, 0), \quad W(0, 1|0, 1),$$
$$W(0, 0|0, 0), \quad W(1, 1| -1, -1), \quad W(1, 1|0, 0), \quad W(1, 0|0, -1).$$
$$(2.4)$$

The first five amplitudes are helicity nonflip and the last three are helicity flip. It is noted that the s-channel helicity-nonflip amplitudes are semipositive, but not the helicity-flip ones.

In our previous works [41,42], we have applied the Cauchy-Schwarz inequality [54,55] to the above photon helicity amplitudes and have derived a positivity bound:

$$|W(a, b|a', b')| \leq \sqrt{W(a, b|a, b)W(a', b'|a', b')}. \quad (2.5)$$

Writing down explicitly, we obtain the following three positivity constraints:

$$|W(1, 1| -1, -1)| \leq W(1, 1|1, 1), \quad (2.6)$$

$$|W(1, 1|0, 0)| \leq \sqrt{W(1, 1|1, 1)W(0, 0|0, 0)}, \quad (2.7)$$

$$|W(1, 0|0, -1)| \leq \sqrt{W(1, 0|1, 0)W(0, 1|0, 1)}. \quad (2.8)$$

The photon-photon scattering phenomenology is often discussed in terms of the photon structure functions instead of the s-channel helicity amplitudes. Budnev, Chernyak, and Ginzburg (BCG) [37] introduced the following eight independent structure functions, in terms of which the absorptive part of virtual photon-photon forward scattering, $W^{\mu\nu\rho\sigma}$, is written as (See Appendix A)
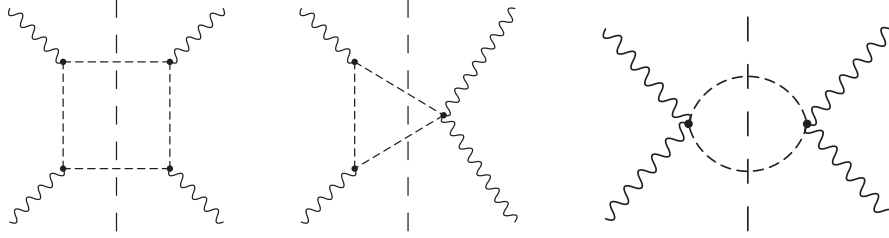
FIG. 2.   Squark-loop diagrams (box, triangle, bubble) contribution to photon structure functions.

$$W_{\mu\nu\rho\sigma} = (T_{TT})_{\mu\nu\rho\sigma}W_{TT} + (T_{TT}^a)_{\mu\nu\rho\sigma}W_{TT}^a$$
$$+ (T_{TT}^\tau)_{\mu\nu\rho\sigma}W_{TT}^\tau + (T_{LT})_{\mu\nu\rho\sigma}W_{LT}$$
$$+ (T_{TL})_{\mu\nu\rho\sigma}W_{TL} + (T_{LL})_{\mu\nu\rho\sigma}W_{LL}$$
$$- (T_{TL}^\tau)_{\mu\nu\rho\sigma}W_{TL}^\tau - (T_{TL}^{\tau a})_{\mu\nu\rho\sigma}W_{TL}^{\tau a}, \quad (2.9)$$

where T_i's are the projection operators given in Appendix A.

The virtual photon structure functions W_i's are functions of three invariants, i.e., $p \cdot q$, $q^2 (= -Q^2)$, and $p^2 (= -P^2)$, and have no kinematical singularities. The subscripts "T" and "L" refer to the transverse and longitudinal photon, respectively. The structure functions with the superscript "τ" correspond to transitions with spin flip for each of the photons with total helicity conservation, while those with the superscript "a" correspond to the $\mu\nu$ antisymmetric part of $W_{\mu\nu\rho\sigma}$ and are measured, for example, through the two-photon processes in polarized e^+e^- collision experiments. These eight structure functions are related to the s-channel helicity amplitudes as follows [37]:

$$W_{TT} = \tfrac{1}{2}[W(1, 1|1, 1) + W(1, -1|1, -1)],$$
$$W_{LT} = W(0, 1|0, 1),$$
$$W_{TL} = W(1, 0|1, 0),$$
$$W_{LL} = W(0, 0|0, 0),$$
$$W_{TT}^a = \tfrac{1}{2}[W(1, 1|1, 1) - W(1, -1|1, -1)], \quad (2.10)$$
$$W_{TT}^\tau = W(1, 1| - 1, -1),$$
$$W_{TL}^\tau = \tfrac{1}{2}[W(1, 1|0, 0) - W(1, 0|0, -1)],$$
$$W_{TL}^{\tau a} = \tfrac{1}{2}[W(1, 1|0, 0) + W(1, 0|0, -1)].$$

Since the helicity-nonflip amplitudes are non-negative, the first four structure functions are positive semidefinite and the last four are not. Because of the fact that the absorptive part $W_{\mu\nu\rho\sigma}(p, q)$ is symmetric under the simultaneous interchange of $\{q, \mu, \nu\} \leftrightarrow \{p, \rho, \sigma\}$, all the virtual photon structure functions, except W_{LT} and W_{TL}, are symmetric under interchange of $p \leftrightarrow q$, while $W_{LT}(p \cdot q, q^2, p^2) = W_{TL}(p \cdot q, p^2, q^2)$. In terms of these structure functions, the positivity constraints (2.6), (2.7), and (2.8) are rewritten as

$$|W_{TT}^\tau| \le (W_{TT} + W_{TT}^a), \quad (2.11)$$

$$|W_{TL}^\tau + W_{TL}^{\tau a}| \le \sqrt{(W_{TT} + W_{TT}^a)W_{LL}}, \quad (2.12)$$

$$|W_{TL}^\tau - W_{TL}^{\tau a}| \le \sqrt{W_{TL}W_{LT}}. \quad (2.13)$$

In fact, the following bounds,

$$|W_{TT}^\tau| \le 2W_{TT}, \qquad 2(W_{TL}^\tau)^2 \le 2W_{LL}W_{TT} + W_{TL}W_{LT}, \quad (2.14)$$

were derived, some time ago, from the positiveness of the $\gamma\gamma$ cross section for arbitrary photon polarization [56]. Note that the constraints (2.11), (2.12), and (2.13) which we have obtained are more stringent than the above ones (2.14).

III. CALCULATION OF SQUARK CONTRIBUTION AND THE RESULTS

The structure functions are evaluated by multiplying the relevant projection operator to the structure tensor $W_{\mu\nu\rho\sigma}$ which is the imaginary part of the forward photon-photon amplitude $T_{\mu\nu\rho\sigma}$:

$$W_i = P_i^{\mu\nu\rho\sigma} \frac{1}{\pi} \mathrm{Im} T_{\mu\nu\rho\sigma} = \int dPS^{(2)} P_i^{\mu\nu\rho\sigma} \mathcal{M}_{\mu\rho}^* \mathcal{M}_{\nu\sigma}, \quad (3.1)$$

where P_i's are the normalized projection operators defined in Appendix A. In our calculation, we evaluated the structure functions by two methods: (i) computing the discontinuity of the forward photon-photon amplitude (see Fig. 2) multiplied by projection operators, and (ii) integrating the squared amplitudes $\mathcal{M}_{\mu\rho}^* \mathcal{M}_{\nu\sigma}$ for the squark $\tilde{q}$ and anti-squark $\bar{\tilde{q}}$ production $\gamma + \gamma \rightarrow \tilde{q} + \bar{\tilde{q}}$, multiplied by projection operators over the two-body phase space $dPS^{(2)}$. Both calculations coincide for the eight structure functions.

We have summarized our results for the eight virtual structure functions in Appendix B. Here we present the expressions converted to the structure functions usually used for the nucleon target in the following.

We note that the virtual photon structure functions F_1^γ, F_2^γ, F_L^γ, g_1^γ, and g_2^γ are related to the ones introduced by BCG in [37] as follows:

$$F_1^\gamma(x, Q^2, P^2) = W_{TT} - \frac{1}{2} W_{TL},$$

$$F_2^\gamma(x, Q^2, P^2) = \frac{x}{\tilde{\beta}^2}\left[W_{TT} + W_{LT} - \frac{1}{2} W_{LL} - \frac{1}{2} W_{TL}\right],$$

$$F_L^\gamma(x, Q^2, P^2) = F_2^\gamma - xF_1^\gamma, \tag{3.2}$$

$$g_1^\gamma(x, Q^2, P^2) = \frac{1}{\tilde{\beta}^2}[W_{TT}^a - \sqrt{1 - \tilde{\beta}^2} W_{TL}^{\tau a}],$$

$$g_2^\gamma(x, Q^2, P^2) = -\frac{1}{\tilde{\beta}^2}\left[W_{TT}^a - \frac{1}{\sqrt{1 - \tilde{\beta}^2}} W_{TL}^{\tau a}\right],$$

where independent variables are $x = Q^2/2p \cdot q$ (Bjorken variable), P^2, Q^2, and m^2. Here we have introduced the variable $\tilde{\beta}$ given as

$$\tilde{\beta} = \sqrt{1 - \frac{P^2 Q^2}{(p \cdot q)^2}} = \sqrt{1 - \frac{4x^2 P^2}{Q^2}}. \tag{3.3}$$

In order to write down above structure functions, we also introduce the following variables:

$$\beta = \sqrt{1 - \frac{4m^2}{(p + q)^2}} = \sqrt{1 + \frac{4m^2 x}{xP^2 + (x - 1)Q^2}}, \tag{3.4}$$

$$L = \ln\frac{1 + \beta\tilde{\beta}}{1 - \beta\tilde{\beta}}. \tag{3.5}$$

One of the characteristics of the squark diagrams, W_{LT} and W_{TL} do not receive any contribution from the triangle and bubble diagrams which consist of seagull graphs [45].

For a flavor q, the structure functions turn out to be

$$\begin{aligned}
F_1^\gamma = N_c \frac{\alpha}{\pi} e_q^4 \Bigg[& -\frac{1}{\tilde{\beta}^3} L \Bigg\{ -8\tilde{\beta}^2 \frac{m^4}{Q^4} x^2 + \frac{m^2}{Q^2}\bigg[(1 - \tilde{\beta}^2)^2 \\
& + \frac{1}{2}(1 - \tilde{\beta}^2)(12x^2 - 4x - 3) + 4x(1 - 2x)\bigg] \\
& + \frac{1}{8}\frac{P^2}{Q^2}((1 - \tilde{\beta}^2) + 4x^2 - 4x)((1 - \tilde{\beta}^2) + 8x^2 - 2)\Bigg\} \\
& + \frac{\beta}{\tilde{\beta}^2}\Bigg\{\frac{P^2}{Q^2} x(1 - 3x) + \frac{4m^2}{Q^2} x(1 - x) \\
& - \frac{1}{4x}(1 - \tilde{\beta}^2)\bigg[(1 - x)(1 - \tilde{\beta}^2) + x\tilde{\beta}^2 \frac{P^2}{Q^2}\bigg] \\
& - 2x(1 - x) + 1\Bigg\}\Bigg], \tag{3.6}
\end{aligned}$$

$$\begin{aligned}
F_2^\gamma = N_c \frac{\alpha}{\pi} e_q^4 x \Bigg[& \frac{1}{\tilde{\beta}^5} L \Bigg\{ 8\tilde{\beta}^2 \frac{m^4}{Q^4} x^2 + \frac{m^2}{Q^2}\bigg[\frac{1}{2}(1 - \tilde{\beta}^2)(-12x^2 - 4x + 3) + 4x(3x - 1)\bigg] + \frac{1}{8}\frac{P^2}{Q^2}(1 - \tilde{\beta}^2)^2 \\
& + \frac{1}{4}\frac{P^2}{Q^2}(1 - \tilde{\beta}^2)(2x^2 - 2x + 1) - \frac{P^2}{Q^2} x(2x(2x^2 - 2x + 1) + 1) + 2x(1 - x)\Bigg\} \\
& + \frac{\beta}{2\tilde{\beta}^4(1 - \beta^2\tilde{\beta}^2)}\Bigg\{ 2(\beta^2 - 1)\tilde{\beta}^2 \frac{m^2}{Q^2}[(1 - \tilde{\beta}^2) - 4x(1 - x)] + 2(1 - \beta^2)\bigg[\frac{P^2}{Q^2}(1 - \tilde{\beta}^2)^2 \\
& + \frac{1}{4}\frac{P^2}{Q^2}(1 - \tilde{\beta}^2)(12x^2 - 28x - 1) + \frac{P^2}{Q^2} x(1 - x)(2x + 1)(10x + 1) - 8x(1 - x) + 1\bigg] \\
& + (1 - \tilde{\beta}^2)\bigg[-\frac{3}{2}\frac{P^2}{Q^2}(1 - \tilde{\beta}^2) + \frac{2P^2}{Q^2} x(x + 3) + (12x^2 - 12x + 1)\bigg]\Bigg\}\Bigg], \tag{3.7}
\end{aligned}$$

$$\begin{aligned}
F_L^\gamma = N_c \frac{\alpha}{\pi} e_q^4 \Bigg[& -\frac{1}{2\tilde{\beta}^3} L(2x - 1 + \tilde{\beta}^2)\Bigg\{\frac{1}{4}(1 - \tilde{\beta}^2)(4x - 1) - \frac{4m^2}{Q^2} x^2 + \frac{1}{2}(1 - \tilde{\beta}^2)\bigg[(1 - x)(1 - \tilde{\beta}^2) + x\tilde{\beta}^2 \frac{P^2}{Q^2}\bigg] \\
& - 2x(1 - x)\Bigg\} + \frac{2\beta x}{\tilde{\beta}^2(1 - \beta^2\tilde{\beta}^2)}\Bigg\{-\frac{m^2}{Q^2}[(1 - \tilde{\beta}^2)^2 - 4(1 - \tilde{\beta}^2)x(2x + 1) + 12x^2] \\
& - \frac{P^2}{Q^2}\bigg[\frac{1}{4}(1 - \tilde{\beta}^2)^2 - (1 - \tilde{\beta}^2)x(2x + 1) + x^2 + 8x^3(1 - x)\bigg]\Bigg\}\Bigg], \tag{3.8}
\end{aligned}$$

$$\begin{aligned}
g_1^\gamma = N_c \frac{\alpha}{\pi} e_q^4 \Bigg[& \frac{1}{\tilde{\beta}^5} L \Bigg\{\frac{2m^2 x}{Q^2}[(1 - \tilde{\beta}^2)^2 - 3(1 - \tilde{\beta}^2) + 2] + \frac{P^2}{Q^2} x\bigg[\frac{1}{2}(1 - \tilde{\beta}^2)^2 + 2(1 - \tilde{\beta}^2)(x^2 - 1) - 2x(4x - 3)\bigg]\Bigg\} \\
& + \frac{\beta}{\tilde{\beta}^4}\Bigg\{\frac{P^2}{Q^2} x(1 - \tilde{\beta}^2) + \frac{2P^2 x}{Q^2}(2x^2 - 4x + 1) + (2x - 1)\Bigg\}\Bigg], \tag{3.9}
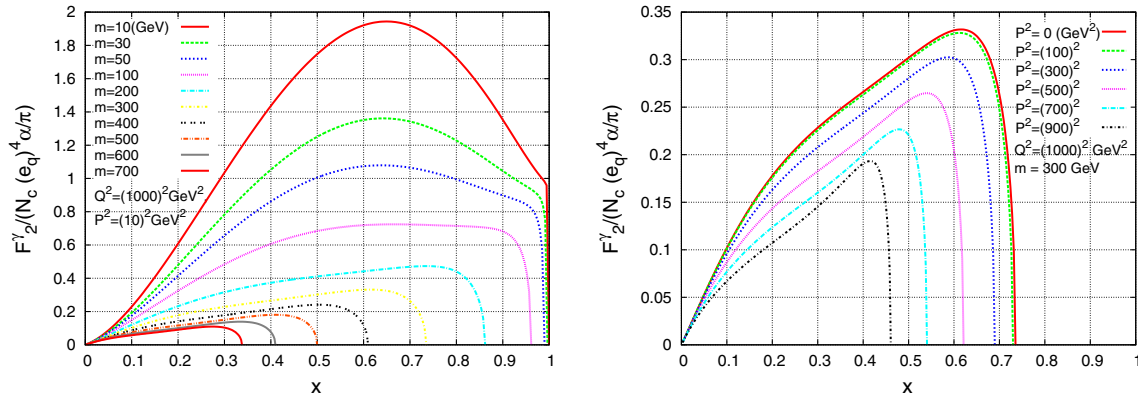\end{aligned}$$

FIG. 3 (color online). F_2^γ as a function of x for various values of squark mass, m, which are given in units of GeV, for fixed $P^2 = (10)^2$ GeV^2 and $Q^2 = (1000)^2$ GeV^2 (left), and for various P^2 in units of GeV^2 with $m = 300$ GeV (right).
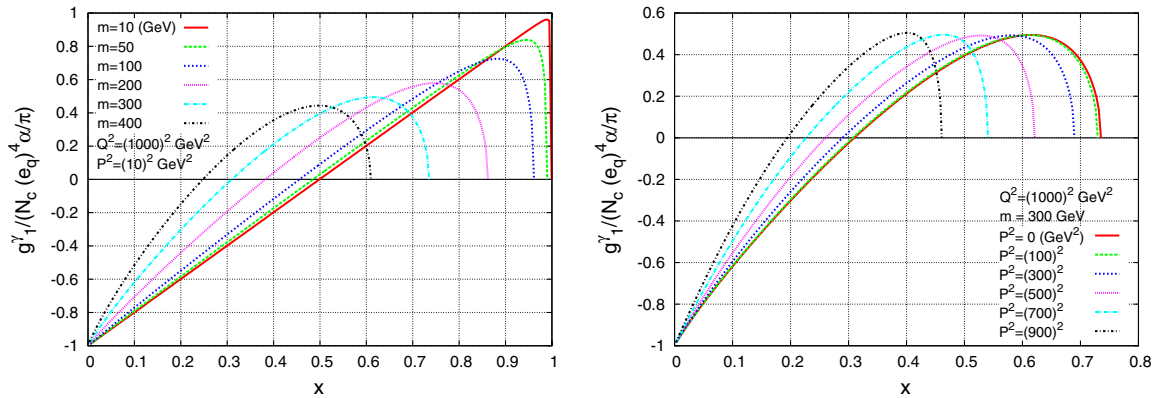

FIG. 4 (color online). g_1^γ for various squark mass m in units of GeV (left), and for various P^2 in units of GeV^2 with fixed $Q^2 = (1000)^2$ GeV^2 and $m = 300$ GeV (right).

$$g_2^\gamma = N_c \frac{\alpha}{\pi} e_q^4 \left[\frac{1}{2\tilde{\beta}^2} L \left\{ \frac{P^2}{Q^2} 2x(2x^2 - 4x + 1) - \frac{4m^2 x}{Q^2} \right. \right.$$

$$\left. + (1 - \tilde{\beta}^2) \left[(1-x)(1-\beta^2) + x\beta^2 \frac{P^2}{Q^2} \right] + (2x-1) \right\}$$

$$\left. + \frac{\beta}{\tilde{\beta}^4} \left\{ \frac{P^2}{Q^2} x(4x - 3) + (2 - 3x) \right\} \right], \qquad (3.10)$$

where $\alpha = e^2/4\pi$ is the fine structure constant of QED, N_c is the number of colors, $N_c = 3$ for supersymmetric QCD. e_q is the electric charge of squark of qth flavor. In order to take into account all the flavor contributions we have to sum over flavors $\sum_q$.

We should note that the variables L, β, and $\tilde{\beta}$ are not independent of the variables x, P^2, Q^2, and m^2, the expressions given here are not unique. Also we should note that these structure functions do not depend on the dimensionful variables Q^2, P^2, and m^2, but they depend only on the ratios, P^2/Q^2 and m^2/Q^2.

We plot in Figs. 3–6 squark contributions to the photon structure functions as functions of x. The vertical axes are in units of $N_c \frac{\alpha}{\pi} e_q^4$, where N_c is the number of colors, $N_c = 3$ for supersymmetric QCD. e_q is the electric charge

of the squark which is the superpartner of the quark of the qth flavor.

In these plots we have chosen $Q^2 = (1000)^2$ GeV^2, and $P^2 = (10)^2$ GeV^2. The allowed x region is $0 \le x \le x_{\max}$ with

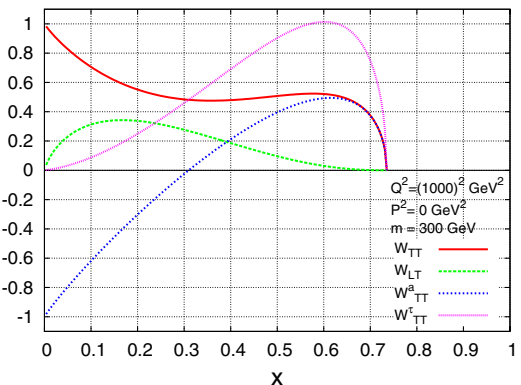$$x_{\max} = \frac{1}{1 + \frac{P^2}{Q^2} + \frac{4m^2}{Q^2}}. \qquad (3.11)$$

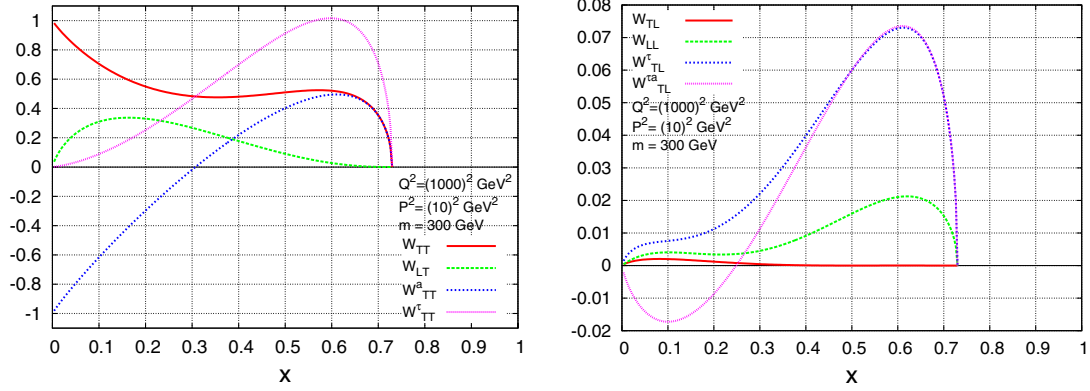FIG. 5 (color online). Four real photon structure functions: W_{TT}, W_{LT}, W_{TT}^a, W_{TT}^τ.

FIG. 6 (color online).   Eight virtual photon structure functions:W_{TT}, W_{LT}, W^a_{TT}, W^τ_{TT} (left), W_{TL}, W_{LL}, W^τ_{TL}, $W^{\tau a}_{TL}$ (right). The values of P^2 and Q^2 are in units of GeV^2.

The photon structure functions can be classified into two groups: (i) W_{TT}, W_{LT}, W^a_{TT}, W^τ_{TT} and (ii) W_{TL}, W_{LL}, W^τ_{TL}, $W^{\tau a}_{TL}$. The first group also exists for the real photon target, while the second group does not exist for the real photon case and are small in magnitude compared to the first group. The graphs show that all the structure functions tend to vanish as $x \rightarrow x_{\max}$ which is the kinematical constraint.

Positivity and equality

The positivity constraints (2.11) and (2.13) derived from the general Cauchy-Schwarz inequalities in fact lead to the following equalities for the squark contributions:

$$W^\tau_{TT} = W_{TT} + W^a_{TT}, \tag{3.12}$$

$$|W^\tau_{TL} - W^{\tau a}_{TL}| = \sqrt{W_{TL}W_{LT}}, \tag{3.13}$$

while we have an inequality

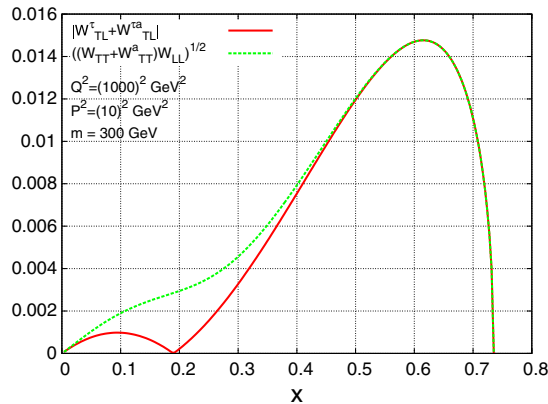$$|W^\tau_{TL} + W^{\tau a}_{TL}| \le \sqrt{(W_{TT} + W^a_{TT})W_{LL}}. \tag{3.14}$$

FIG. 7   (color   online).   Inequality   (3.14)   for $Q^2 =$ (1000)^2 GeV^2, $P^2 = $ (10)^2 GeV^2 and $m = 300$ GeV.

The first equality (3.12) can be rewritten in terms of the helicity amplitudes as

$$W(1, 1| - 1, -1) = W(1, 1|1, 1), \tag{3.15}$$

which holds both for the real ($P^2 = 0$) and virtual ($P^2 \ne 0$) photon target. We can also read off this relation from Figs. 5 and 6. In the limit $x \rightarrow 0$, for example, $W_{TT} \rightarrow 1$, while $W^a_{TT} \rightarrow -1$ and, hence, $W^\tau_{TT} \rightarrow 0$. Note that because of Eq. (3.15), $W(1, 1| - 1, -1)$ or W^τ_{TT} is positive definite, and the left-hand side of (3.12) is without an absolute value symbol.

The second equality (3.13) only exists for the virtual photon case. One can also see that this relation holds from Fig. 6, where W^τ_{TL} almost overlaps with $W^{\tau a}_{TL}$ at larger x for which the product $W_{TL}W_{LT}$ looks very small, while in the smaller x region the difference $W^\tau_{TL} - W^{\tau a}_{TL}$ becomes sizable and the product $W_{TL}W_{LT}$ shows nonvanishing values.

The inequality (3.14) is illustrated in Fig. 7.

IV. REAL PHOTON CASE

We now consider the real photon case of the above structure functions by taking the limit: $P^2 \rightarrow 0$ or $\tilde{\beta} \rightarrow 1$. Then the number of the independent structure functions reduces to four for the real photon target. They are W_{TT}, W_{LT}, W^τ_{TT}, and W^a_{TT} given as follows:

$$W_{TT} = N_c \frac{\alpha}{\pi} e^4_q \left[L\tau x \left\{ \frac{1}{2} \tau x + (2x - 1) \right\} + \beta \{ \tau x(1 - x) \right.$$
$$\left. + 2x^2 - 2x + 1 \} \right], \tag{4.1}$$

$$W_{LT} = N_c \frac{\alpha}{\pi} e^4_q [L\{\tau x^2 + 2x(1 - x)\} - 6\beta x(1 - x)], \tag{4.2}$$

$$W^a_{TT} = N_c \frac{\alpha}{\pi} e^4_q [L\tau x + \beta(2x - 1)], \tag{4.3}$$

$$W_{TT}^{\tau} = N_c \frac{\alpha}{\pi} e_q^4 \left[L\left\{ 2\tau\left(1 + \frac{1}{4}\tau\right)x^2 \right\} + \beta\{2x^2 + \tau x(1-x)\} \right],$$
(4.4)

where the logarithmic term L, the mass-ratio parameter τ, and the velocity variable β are defined for the real photon case as

$$L = \ln\frac{1+\beta}{1-\beta}, \qquad \tau = \frac{4m^2}{Q^2}, \qquad \beta = \sqrt{1 - \frac{\tau x}{(1-x)}},$$
(4.5)

which are different from L and β for the virtual photon case. Note that from the above equation the following relation holds:

$$(1-x)(1-\beta^2) = \tau x.$$
(4.6)

In terms of these four structure functions we can derive the usual structure functions F_1^{γ}, F_2^{γ}, F_L^{γ}, and g_1^{γ} as follows:

$$F_1^{\gamma} = N_c \frac{\alpha}{\pi} e_q^4 \left[L\left\{ \frac{1}{2}\tau^2 x^2 + \tau x(2x-1) \right\} + \beta\{\tau x(1-x) \right.$$
$$\left. + 2x^2 - 2x + 1\} \right],$$
(4.7)

$$F_2^{\gamma} = N_c \frac{\alpha}{\pi} e_q^4 x \left[L\left\{ \frac{1}{2}\tau^2 x^2 + \tau x(3x-1) + 2x(1-x) \right\} \right.$$
$$\left. + \beta\{\tau x(1-x) + 8x^2 - 8x + 1\} \right],$$
(4.8)

$$F_L^{\gamma} = N_c \frac{\alpha}{\pi} e_q^4 x[L\{\tau x^2 + 2x(1-x)\} + 6\beta(x^2 - x)],$$
(4.9)

$$g_1^{\gamma} = N_c \frac{\alpha}{\pi} e_q^4 [L\tau x + \beta(2x-1)].$$
(4.10)

Note that we have the following relation:

$$F_L^{\gamma} = F_2^{\gamma} - xF_1^{\gamma}.$$
(4.11)

Our result for F_2^{γ} for the real photon target (4.8) is consistent with those in Refs. [44–47] and F_L^{γ} in Ref. [45] coincides with our result (4.9). Note that our expression for $F_2^{\gamma}(x, Q^2, P^2)$ with $P^2 \neq 0$ (3.7) is slightly different from that given in Ref. [47].

A. Relation to the splitting functions

It is well known that the collinear singularities in the process of particle emission determine the parton splitting functions and are related to the F_2^{γ} function. Namely, the quark parton distribution function inside the photon reads in the leading logarithmic order

$$q^{\gamma}(x, Q^2) \sim P_{q\gamma}(x) \ln Q^2/m^2,$$
(4.12)

where $P_{q\gamma}$ denotes the photon-quark splitting function. Then the structure function becomes

$$F_{2,q}^{\gamma} \sim N_c \frac{\alpha}{\pi} \sum_q e_q^4 q^{\gamma}(x, Q^2).$$
(4.13)

Similarly for the squark contribution we have

$$F_{2,s}^{\gamma} \sim N_c \frac{\alpha}{\pi} \sum_s e_s^4 s^{\gamma}(x, Q^2),$$
(4.14)

$$s^{\gamma}(x, Q^2) \sim P_{s\gamma}(x) \ln Q^2/m^2,$$
(4.15)

where we note that the splitting functions are given by [57,58]

$$P_{q\gamma}(x) = x^2 + (1-x)^2,$$
$$P_{s\gamma}(x) = 1 - \{x^2 + (1-x)^2\} = 2x(1-x),$$
(4.16)

for which the following relation holds:

$$P_{q\gamma}(x) + P_{s\gamma}(x) = 1.$$
(4.17)

B. Mass singularities of the structure functions

Let us consider the massless limit of the real photon structure functions. Ignoring the power correction of m^2/Q^2, the photon structure functions become

$$F_1^{\gamma} = W_{TT} \sim N_c \frac{\alpha}{\pi} e_q^4 \{2x^2 - 2x + 1\},$$
(4.18)

$$F_2^{\gamma} = x[W_{TT} + W_{LT}] \sim N_c \frac{\alpha}{\pi} e_q^4 x \left[2x(1-x) \ln\left(\frac{Q^2}{m^2}\frac{1-x}{x}\right) \right.$$
$$\left. + 8x^2 - 8x + 1 \right],$$
(4.19)

$$F_L^{\gamma} = xW_{LT} \sim N_c \frac{\alpha}{\pi} e_q^4 x \left[2x(1-x) \ln\left(\frac{Q^2}{m^2}\frac{1-x}{x}\right) \right.$$
$$\left. + 6x(x-1) \right],$$
(4.20)

$$g_1^{\gamma} = W_{TT}^a \sim N_c \frac{\alpha}{\pi} e_q^4 \{2x-1\}.$$
(4.21)

In contrast to the spin $1/2$ quark, mass singularities originate from W_{LT}, while W_{TT} and W_{TT}^a have no such singularities. Note that for the spin $1/2$ quark case, such mass singularities arise in W_{TT} and W_{TT}^a. This can be interpreted as the spinless nature of the squark constituent. In terms of the basis of $F_{1,2,L}^{\gamma}$, the mass singularity appears in F_2^{γ} and F_L^{γ} for the squark case, in contrast to the quark parton case, where mass singularities appear in F_1^{γ} and F_2^{γ}. Because of the logarithmic term due to mass singularities of F_L^{γ}, the squark contribution to F_L^{γ} is sizable compared to that for F_2^{γ}.

C. Inequality $|g_1^{\gamma}| \leq F_1^{\gamma}$

For the real photon

$$g_1^{\gamma} = W_{TT}^a = \tfrac{1}{2}[W(1, 1|1, 1) - W(1, -1|1, -1)],$$
(4.22)

$$F_1^{\gamma} = W_{TT} = \tfrac{1}{2}[W(1, 1|1, 1) + W(1, -1|1, -1)].$$
(4.23)

Since the helicity nonflip amplitudes $W(1, 1|1, 1)$ and $W(1, -1|1, -1)$ are semipositive definite, we are led to the inequality:
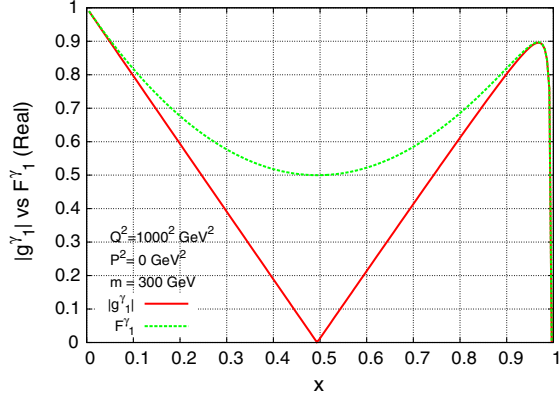
FIG. 8 (color online).   The inequality: $|g_1^\gamma| \le F_1^\gamma$ for the real photon target in the case of $Q^2 = (1000)^2$ GeV^2 and $m = 300$ GeV.

$$|g_1^\gamma| \le F_1^\gamma, \qquad (4.24)$$

which holds both for the squark and quark contribution. This can be shown in Fig. 8.

We have also numerically studied the above inequality for the virtual photon case and it has turned out that the inequality is not satisfied at the small x region for the case where P^2 is much bigger than m^2.

D. g_1^γ sum rule

For the squark contribution the first moment of the g_1^γ structure functions turns out to be

$$\int_0^{x_{\max}} g_1^\gamma(x, Q^2) dx$$

$$= N_c \frac{\alpha}{\pi} e_q^4 \left[\int_0^{x_{\max}} \tau x L dx + \int_0^{x_{\max}} \beta(2x-1) dx \right], \quad (4.25)$$

where

$$\tau = \frac{4m^2}{Q^2}, \qquad x_{\max} = \frac{1}{1+\tau}. \qquad (4.26)$$

Now by repeated use of integration by parts, where we get vanishing boundary terms, the first and the second integrals are found to be

$$\text{1st term} = \int_0^{x_{\max}} \tau x L dx$$

$$= \tau \frac{x^2}{2} L \Big|_0^{x_{\max}} - \int_0^{x_{\max}} \tau \frac{x^2}{2} \frac{d}{dx} \ln\left(\frac{1+\beta}{1-\beta}\right) dx$$

$$= -\tau x^2 \frac{\beta(x)}{1-\beta^2} \Big|_0^{x_{\max}} + \tau \int_0^{x_{\max}} \beta(x) \frac{d}{dx}\left(\frac{x^2}{1-\beta^2}\right) dx$$

$$= -\int_0^{x_{\max}} \beta(2x-1) dx$$

$$= -\frac{\tau}{2(\tau+1)} + \frac{\tau(\tau+1)\log(\frac{\sqrt{\tau+1}+1}{\sqrt{\tau}})}{2(\tau+1)^{3/2}}, \qquad (4.27)$$

$$\text{2nd term} = \int_0^{x_{\max}} \beta(2x-1) dx$$

$$= \frac{\tau}{2(\tau+1)} - \frac{\tau(\tau+1)\log(\frac{\sqrt{\tau+1}+1}{\sqrt{\tau}})}{2(\tau+1)^{3/2}}. \qquad (4.28)$$

Therefore the first and the second terms cancel with each other and we end up with

$$\int_0^{x_{\max}} g_1^\gamma(x, Q^2) dx = 0. \qquad (4.29)$$

For the quark contribution we have

$$\int_0^{x_{\max}} (2x-1) L dx = -\frac{1}{\tau+1} - \frac{\tau \log(\frac{\sqrt{\tau+1}+1}{\sqrt{\tau}})}{(\tau+1)^{3/2}}, \quad (4.30)$$

$$\int_0^{x_{\max}} \beta(-4x+3) dx = \frac{1}{\tau+1} + \frac{\tau \log(\frac{\sqrt{\tau+1}+1}{\sqrt{\tau}})}{(\tau+1)^{3/2}}. \quad (4.31)$$

Hence, we find 1st + 2nd = 0. Thus the first moment of the g_1^γ structure function for the real photon target vanishes both for the squark and quark case.

V. SQUARK SIGNATURE IN W_{TT}^τ

Among the eight virtual photon structure functions, W_{TT}^τ, which is nothing but a spin-flip helicity amplitude $W(1, 1| -1, -1)$, shows quite different behaviors between squark and quark constituents. Namely, the squark gives a positive contribution while the quark contributes negative values for the structure function. If we consider the ideal case where the quark and its superpartner have the same mass, then we have the following relation for the virtual photon and its real photon limit:

$$W_{TT}^\tau|_{\text{squark}} + W_{TT}^\tau|_{\text{quark}} = N_c \frac{\alpha}{\pi} e_q^4 \frac{1-\tilde\beta^2}{\tilde\beta} L \to 0 \quad (P^2 \to 0).$$

$$(5.1)$$

Namely, in the real photon case, both contributions to W_{TT}^τ exactly cancel each other.

In Fig. 9 we have plotted the behavior of W_{TT}^τ for the six flavor quarks with their masses properly taken into account, as well as one squark which gives positive contribution. Here we have taken the squark's electric charge to be 2/3 and mass 900 GeV as an illustration. Note that the signal of the presence of the squark appears as a positive swelling or bump at small x, where the quark contributions are negligibly small.[1]

---

[1]W_{TT}^τ can be experimentally measured from the dependence of the cross section on the azimuthal angle between the scattering planes of the electron and positron in the photon center-of-mass frame [38].
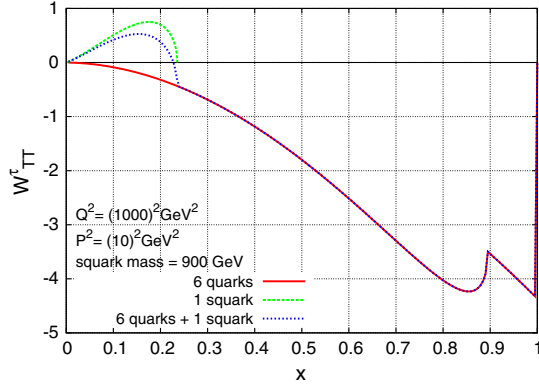
FIG. 9 (color online). W_{TT}^τ for a squark with mass 900 GeV (short-dashed curve) and that for the six quarks with masses properly taken into account (solid curve) as well as the total contribution (dotted curve). At around $x \sim 0.9$ there exists a kink structure due to the threshold behavior of the top quark. At small x we find the positive swelling or bump as a signature of the squark contribution.

VI. CONCLUSION

In this paper, we have evaluated eight virtual photon structure functions arising from squark parton contribution, which have been unknown so far. From a general argument based on Cauchy- Schwarz inequality, we can derive the three positivity constraints on the helicity amplitudes which can then be translated into those on structure functions. Now remarkably, for the squark contribution, these three constraints turn out to be two equalities and one inequality.

For the case of the real photon target, we obtained the vanishing first moment sum rule for the g_1^γ structure function, which is also realized in the case of spin 1/2 quark parton contribution. Similarly we have confirmed that the positivity bound $|g_1^\gamma| \leq F_1^\gamma$ holds for the squark parton as in the quark parton case. Mass singularities of the structure function appear in W_{LT} for the case of squark, in contrast to the case of quark parton where they appear in W_{TT} and W_{TT}^a. This can be interpreted as the spinless nature of squark constituent.

We are particularly interested in the W_{TT}^τ structure function for which the behavior of the squark is quite different from that of the quark. Namely, the squark gives a positive contribution while the quark contributes negative values for the structure function. The signature of the squark could be a positive swelling or bump at small x, where the quark contributions are negligibly small. In the ideal limit where both squark and quark possess the same mass, their contributions exactly cancel each other. This situation might be understood from the supersymmetric relation.

In our numerical analysis, the kinematic parameters we have chosen for the Q^2, P^2, and m^2 are just the illustrative values and do not necessarily correspond to the realistic

values in the ILC region. However, the parameters can be freely scaled up or scaled down since we have general formulas for the structure functions, which only depend on the ratios such as m^2/Q^2, P^2/Q^2. The heavy squark mass, m, could be set larger than 1 TeV as the recently reported results from the ATLAS/CMS group at LHC.

In this paper we have studied squark contributions to the photon structure functions only through the QED interaction paying particular attention to the heavy mass effects. The logarithmic Q^2 dependence due to the supersymmetric QCD radiative effects can be incorporated by the DGLAP-type evolution equation with the suitable boundary condition taking into account the mass effects [59]. This will be discussed in the future publication.

APPENDIX A: PROJECTION OPERATORS

In general, taking into account P, T, and gauge invariance, the tensor $W^{\mu\nu\rho\sigma}$ can be expressed in terms of the eight independent photon structure functions as follows:

$$\begin{aligned} W^{\mu\nu\rho\sigma} = &(T_{TT})^{\mu\nu\rho\sigma} W_{TT} + (T_{TT}^a)^{\mu\nu\rho\sigma} W_{TT}^a \\ &+ (T_{TT}^\tau)^{\mu\nu\rho\sigma} W_{TT}^\tau + (T_{LT})^{\mu\nu\rho\sigma} W_{LT} \\ &+ (T_{TL})^{\mu\nu\rho\sigma} W_{TL} + (T_{LL})^{\mu\nu\rho\sigma} W_{LL} \\ &- (T_{TL}^\tau)^{\mu\nu\rho\sigma} W_{TL}^\tau - (T_{TL}^{\tau a})^{\mu\nu\rho\sigma} W_{TL}^{\tau a}, \end{aligned} \quad \text{(A1)}$$

where T_i's are the projection operators given by

$$(T_{TT})^{\mu\nu\rho\sigma} = R^{\mu\nu} R^{\rho\sigma}, \quad \text{(A2a)}$$

$$(T_{TL})^{\mu\nu\rho\sigma} = R^{\mu\nu} k_2^\rho k_2^\sigma, \quad \text{(A2b)}$$

$$(T_{LT})^{\mu\nu\rho\sigma} = k_1^\mu k_1^\nu R^{\rho\sigma}, \quad \text{(A2c)}$$

$$(T_{LL})^{\mu\nu\rho\sigma} = k_1^\mu k_1^\nu k_2^\rho k_2^\sigma, \quad \text{(A2d)}$$

$$(T_{TT}^a)^{\mu\nu\rho\sigma} = R^{\mu\rho} R^{\nu\sigma} - R^{\mu\sigma} R^{\nu\rho}, \quad \text{(A2e)}$$

$$(T_{TT}^\tau)^{\mu\nu\rho\sigma} = \tfrac{1}{2}(R^{\mu\rho} R^{\nu\sigma} + R^{\mu\sigma} R^{\nu\rho} - R^{\mu\nu} R^{\rho\sigma}), \quad \text{(A2f)}$$

$$\begin{aligned} (T_{TL}^\tau)^{\mu\nu\rho\sigma} = &R^{\mu\rho} k_1^\nu k_2^\sigma + R^{\mu\sigma} k_1^\nu k_2^\rho + k_1^\mu k_2^\rho R^{\nu\sigma} \\ &+ k_1^\mu k_2^\sigma R^{\nu\rho}, \end{aligned} \quad \text{(A2g)}$$

$$\begin{aligned} (T_{TL}^{\tau a})^{\mu\nu\rho\sigma} = &R^{\mu\rho} k_1^\nu k_2^\sigma - R^{\mu\sigma} k_1^\nu k_2^\rho + k_1^\mu k_2^\rho R^{\nu\sigma} \\ &- k_1^\mu k_2^\sigma R^{\nu\rho}, \end{aligned} \quad \text{(A2h)}$$

with

$$R^{\mu\nu} = -g^{\mu\nu} + \frac{1}{X}[p \cdot q(q^\mu p^\nu + q^\nu p^\mu)$$
$$- q^2 p^\mu p^\nu - p^2 q^\mu q^\nu], \tag{A3a}$$

$$k_1^\mu = \sqrt{\frac{-q^2}{X}}\left(p^\mu - \frac{p \cdot q}{q^2} q^\mu\right), \tag{A3b}$$

$$k_2^\mu = \sqrt{\frac{-p^2}{X}}\left(q^\mu - \frac{p \cdot q}{p^2} p^\mu\right), \tag{A3c}$$

and

$$X = (p \cdot q)^2 - p^2 q^2. \tag{A4}$$

The unit vectors k_1, k_2 and the symmetric tensor $R^{\mu\nu}$ which is the metric tensor of the subspace orthogonal to q and p, satisfy the following relations:

$$q \cdot k_1 = p \cdot k_2 = 0,$$
$$k_1^2 = k_2^2 = 1,$$
$$q^\mu R_{\mu\nu} = p^\mu R_{\mu\nu} = k_1^\mu R_{\mu\nu} = k_2^\mu R_{\mu\nu} = 0, \tag{A5}$$
$$R^{\mu\rho} R_\rho^\nu = -R_{\mu\nu},$$
$$R_{\mu\nu} R^{\mu\nu} = -g^{\mu\nu} R_{\mu\nu} = 2.$$

We also introduce

$$x = \frac{Q^2}{2p \cdot q}, \qquad Q^2 = -q^2 > 0, \qquad P^2 = -p^2 > 0, \tag{A6}$$

and

$$\beta = \sqrt{1 - \frac{4m^2}{(p + q)^2}} = \sqrt{1 + \frac{4m^2 x}{xP^2 + (x - 1)Q^2}},$$
$$\tilde{\beta} = \sqrt{1 - \frac{p^2 q^2}{(p \cdot q)^2}} = \sqrt{1 - \frac{4x^2 P^2}{Q^2}}. \tag{A7}$$

The following relations are useful in the practical calculation:

$$\frac{1}{X} = \frac{1}{(p \cdot q)^2 \tilde{\beta}^2},$$
$$k_1 \cdot k_2 = \frac{1}{\sqrt{1 - \tilde{\beta}^2}}, \tag{A8}$$
$$k_1^\mu k_2^\nu = \frac{\sqrt{1 - \tilde{\beta}^2}}{p \cdot q \tilde{\beta}^2}\left(p^\mu - \frac{p \cdot q}{q^2} q^\mu\right)\left(q^\nu - \frac{p \cdot q}{p^2} p^\nu\right).$$

Unless there is any mass scale in addition to p^2, q^2, and $p \cdot q$, the structure functions, which are dimensionless, are eventually written in terms of x and $\tilde{\beta}$.

Using the relations (A5), we obtain the following orthogonality and normalization relations:

$$(T_{TT})^{\mu\nu\rho\sigma}(T_{TT})_{\mu\nu\rho\sigma} = 4, \qquad (T_{TL})^{\mu\nu\rho\sigma}(T_{TL})_{\mu\nu\rho\sigma} = 2,$$
$$(T_{LT})^{\mu\nu\rho\sigma}(T_{LT})_{\mu\nu\rho\sigma} = 2, \qquad (T_{LL})^{\mu\nu\rho\sigma}(T_{LL})_{\mu\nu\rho\sigma} = 1,$$
$$(T_{TT}^a)^{\mu\nu\rho\sigma}(T_{TT}^a)_{\mu\nu\rho\sigma} = 4, \qquad (T_{TT}^\tau)^{\mu\nu\rho\sigma}(T_{TT}^\tau)_{\mu\nu\rho\sigma} = 2,$$
$$(T_{TL}^\tau)^{\mu\nu\rho\sigma}(T_{TL}^\tau)_{\mu\nu\rho\sigma} = 8, \qquad (T_{TL}^{\tau a})^{\mu\nu\rho\sigma}(T_{TL}^{\tau a})_{\mu\nu\rho\sigma} = 8,$$
$$(T_i)^{\mu\nu\rho\sigma}(T_j)_{\mu\nu\rho\sigma} = 0, \quad \text{for } i \neq j.$$

Thus, we get the normalized projection operators [i.e., $(P_{TT})^{\mu\nu\rho\sigma} W_{\mu\nu\rho\sigma} = W_{TT}$ and etc.] which read

$$(P_{TT})^{\mu\nu\rho\sigma} = \tfrac{1}{4}(T_{TT})^{\mu\nu\rho\sigma}, \qquad (P_{TL})^{\mu\nu\rho\sigma} = \tfrac{1}{2}(T_{TL})^{\mu\nu\rho\sigma},$$
$$(P_{LT})^{\mu\nu\rho\sigma} = \tfrac{1}{2}(T_{LT})^{\mu\nu\rho\sigma}, \qquad (P_{LL})^{\mu\nu\rho\sigma} = (T_{LL})^{\mu\nu\rho\sigma},$$
$$(P_{TT}^a)^{\mu\nu\rho\sigma} = \tfrac{1}{4}(T_{TT}^a)^{\mu\nu\rho\sigma}, \qquad (P_{TT}^\tau)^{\mu\nu\rho\sigma} = \tfrac{1}{2}(T_{TT}^\tau)^{\mu\nu\rho\sigma},$$
$$(P_{TL}^\tau)^{\mu\nu\rho\sigma} = -\tfrac{1}{8}(T_{TL}^\tau)^{\mu\nu\rho\sigma}, \qquad (P_{TL}^{\tau a})^{\mu\nu\rho\sigma} = -\tfrac{1}{8}(T_{TL}^{\tau a})^{\mu\nu\rho\sigma}.$$

APPENDIX B: THE EIGHT VIRTUAL PHOTON STRUCTURE FUNCTIONS

$$W_{TT} = N_c \frac{\alpha}{\pi} e_q^4 \left[L \frac{1}{4\tilde{\beta}^5} \frac{1}{x}(1 - \beta^2\tilde{\beta}^2)(4x(1 - x) - 1 + \tilde{\beta}^2)\left\{2x\left(\frac{m^2}{Q^2} - \frac{P^2}{Q^2}(x^2 + x - 1)\right)\right.\right.$$
$$- \frac{1}{2}(1 - \tilde{\beta}^2)\left[(1 - x)(1 - \beta^2) + x\beta^2 \frac{P^2}{Q^2}\right] + (2x - 1)\right\} + \frac{\beta}{\tilde{\beta}^4}\left\{2x\left(\frac{P^2}{Q^2}(2x(x^2 - 4x + 2) - 1) - \frac{2m^2}{Q^2}(x - 1)\right)\right.$$
$$\left. + \frac{1}{2}(1 - \tilde{\beta}^2)\left[\frac{m^2}{Q^2}(8x^2 - 8x - 2) + \frac{P^2}{Q^2}(12x^2 - 8x + 1)\right] + \frac{1}{4}(1 - \tilde{\beta}^2)^2\frac{1}{x}\left[(1 - x)(1 - \beta^2) + x\beta^2 \frac{P^2}{Q^2}\right]\right.$$
$$\left.\left. + (2x^2 - 2x + 1)\right\}\right], \tag{B1}$$

$$W_{TL} = N_c \frac{\alpha}{\pi} e_q^4 2x(1 - 2x)^2 \frac{P^2}{Q^2}\left[-\frac{1}{2\tilde{\beta}^5} L\left\{2x\left(\frac{P^2}{Q^2}(2x^2 - 2x + 1) - \frac{2m^2}{Q^2}\right) + (1 - \tilde{\beta}^2)\left[(1 - x)(1 - \beta^2) + x\beta^2 \frac{P^2}{Q^2}\right]\right.\right.$$
$$\left.\left. + 2(x - 1)\right\} + 3\beta\frac{1}{\tilde{\beta}^4}\left(\frac{P^2}{Q^2}x + (x - 1)\right)\right], \tag{B2}$$

$$W_{LT} = N_c \frac{\alpha}{\pi} e_q^4 \left(1 - \frac{2P^2 x}{Q^2}\right)^2 \left[-\frac{1}{\tilde{\beta}^5} L \left\{ 2x^2 \left(\frac{P^2}{Q^2}(2x^2 - 2x + 1) - \frac{2m^2}{Q^2}\right) + (1 - \tilde{\beta}^2)\left[x(1-x)(1-\beta^2) + x^2\beta^2\frac{P^2}{Q^2}\right]\right.\right.$$
$$\left.\left. - 2x(1-x)\right\} + \frac{6\beta x}{\tilde{\beta}^4}\left(\frac{P^2}{Q^2}x + (x-1)\right)\right], \tag{B3}$$

$$W_{LL} = N_c \frac{\alpha}{\pi} e_q^4 \frac{P^2}{Q^2} x \left[-\frac{1}{\tilde{\beta}^5} L(2x-1)(2x-1+\tilde{\beta}^2)\left(2\frac{P^2}{Q^2}x(2x+3) + 6x - 7\right)\right.$$
$$+ \frac{1}{\tilde{\beta}^4}\frac{8\beta x}{1 - \beta^2\tilde{\beta}^2}\frac{\frac{P^2}{Q^2}x + (x-1)}{(2x-1)^2 - \tilde{\beta}^2}\left\{-2\left[4(x-1)\left(\frac{8m^2 x^2}{Q^2} - (1-\tilde{\beta}^2)x(2x-3)\right) + (1-\tilde{\beta}^2)\right]\right.$$
$$\left. + 2(1-\tilde{\beta}^2)x\left[\frac{8m^2}{Q^2}(4x^2 - 4x - 1) + \frac{P^2}{Q^2}(20x^2 - 20x + 1)\right]\right.$$
$$\left.\left. + 4(1-\tilde{\beta}^2)^2\left[(1-x)(1-\beta^2) + x\beta^2\frac{P^2}{Q^2}\right] + 2x(1-2x)^2\right\}\right], \tag{B4}$$

$$W_{TT}^a = N_c \frac{\alpha}{\pi} e_q^4 \left[\frac{1}{\tilde{\beta}^3} L\left\{-(1-\tilde{\beta}^2)\left[1 - \beta^2(1-x) + x\beta^2\frac{P^2}{Q^2}\right] + \frac{4m^2 x}{Q^2} + 1 - \tilde{\beta}^2\right\} + \frac{\beta}{\tilde{\beta}^2}(2x-1)\left(1 - \frac{2P^2}{Q^2}x\right)\right], \tag{B5}$$

$$W_{TT}^\tau = N_c \frac{\alpha}{\pi} e_q^4 \left[\frac{1}{\tilde{\beta}^5} L\left\{-2x(1-\tilde{\beta}^2)\left[1 - \beta^2(1-x) + x\beta^2\frac{P^2}{Q^2}\right] + 2(1-\beta^2)x(1-x)\right.\right.$$
$$+ \frac{1}{2}(1-\tilde{\beta}^2)(3+\beta^2) + 8x^2 - 6x(1-\tilde{\beta}^2)\right\}\left\{-\frac{P^2}{Q^2}\left[(1-\beta^2)x(1-x) + \frac{1}{4}\beta^2(1-\tilde{\beta}^2) + x^2\right]\right.$$
$$\left. + \frac{m^2}{Q^2} + \frac{P^2}{Q^2}x\right\} + \frac{\beta}{\tilde{\beta}^4}\left\{\frac{1}{4}\frac{P^2}{Q^2}(1-\tilde{\beta}^2)^2 + \frac{1}{2}\frac{P^2}{Q^2}(1-\tilde{\beta}^2)(20x^2 - 12x + 1) + (1-\tilde{\beta}^2)(x^2 - 6x + 2) + 2x^2\right.$$
$$\left.\left. - \frac{1}{4x}\tilde{\beta}^2(1-\beta^2)[4x(1-x) - (1-\tilde{\beta}^2)]\left(\frac{P^2}{Q^2}x + x - 1\right)\right\}\right], \tag{B6}$$

$$W_{TL}^\tau = N_c \frac{\alpha}{\pi} e_q^4 \sqrt{1 - \tilde{\beta}^2}\left[\frac{1}{2\tilde{\beta}^5} L\left(4x\left[\frac{P^2}{Q^2}(2x(x-1)(x-3) - 1) - \frac{2m^2}{Q^2}(x-1)\right] + (1-\tilde{\beta}^2)\left(\frac{m^2}{Q^2}(8x^2 - 8x - 2)\right.\right.\right.$$
$$\left.\left. + \frac{P^2}{Q^2}(8x^2 - 8x + 1)\right) + 2\frac{P^2}{Q^2}x(1-\tilde{\beta}^2)\left[(1-x)(1-\beta^2) + x\beta^2\frac{P^2}{Q^2}\right] + (1-2x)^2\right)$$
$$\left. - \frac{2\beta}{\tilde{\beta}^4}\left(x - 1 + x\frac{P^2}{Q^2}\right)\left(3x - 1 - x(8x-3)\frac{P^2}{Q^2}\right)\right], \tag{B7}$$

$$W_{TL}^{\tau a} = N_c \frac{\alpha}{\pi} e_q^4 \sqrt{1 - \tilde{\beta}^2}\left[-\frac{1}{2\tilde{\beta}^3} L\left\{(1-\tilde{\beta}^2)\left[1 - \beta^2(1-x) + x\beta^2\frac{P^2}{Q^2}\right] - 2x\left(1 + \frac{2m^2 + P^2}{Q^2}\right) + 1\right\}\right.$$
$$\left. - \frac{\beta}{\tilde{\beta}^2}\left\{(x-1) + x\frac{P^2}{Q^2}\right\}\right]. \tag{B8}$$

[1] http://lhc.web.cern.ch/lhc.

[2] http://www.linearcollider.org/cms.

[3] T. F. Walsh, Phys. Lett. **36B**, 121 (1971); S. J. Brodsky, T. Kinoshita, and H. Terazawa, Phys. Rev. Lett. **27**, 280 (1971).

[4] M. Krawczyk, A. Zembrzuski, and M. Staszel, Phys. Rep. **345**, 265 (2001); R. Nisius, Phys. Rep. **332**, 165 (2000); M. Klasen, Rev. Mod. Phys. **74**, 1221 (2002); I. Schienbein, Ann. Phys. (N.Y.) **301**, 128 (2002); R. M. Godbole, Nucl. Phys. Proc. Suppl. **126**, 414 (2004).

[5] T. F. Walsh and P. M. Zerwas, Phys. Lett. **44B**, 195 (1973); R. L. Kingsley, Nucl. Phys. **B60**, 45 (1973).

[6] E. Witten, Nucl. Phys. **B120**, 189 (1977).

[7] W. A. Bardeen and A. J. Buras, Phys. Rev. D **20**, 166 (1979); **21**, 2041(E) (1980).

[8] R. J. DeWitt, L. M. Jones, J. D. Sullivan, D. E. Willen, and H. W. Wyld, Jr., Phys. Rev. D **19**, 2046 (1979); **20**, 1751 (E) (1979).

[9] M. Glück and E. Reya, Phys. Rev. D **28**, 2749 (1983).

[10] S. Moch, J. A. M. Vermaseren, and E. Vogt, Nucl. Phys. **B621**, 413 (2002).

[11] A. Vogt, S. Moch, and J. A. M. Vermaseren, Acta Phys. Pol. B **37**, 683 (2006).

[12] T. Uematsu and T. F. Walsh, Phys. Lett. **101B**, 263 (1981).

[13] T. Uematsu and T. F. Walsh, Nucl. Phys. **B199**, 93 (1982).

[14] G. Rossi, Phys. Rev. D **29**, 852 (1984).

[15] F. M. Borzumati and G. A. Schuler, Z. Phys. C **58**, 139 (1993).

[16] J. Chýla, Phys. Lett. B **488**, 289 (2000).

[17] M. Drees and R. M. Godbole, Phys. Rev. D **50**, 3124 (1994).

[18] M. Glück, E. Reya, and M. Stratmann, Phys. Rev. D **51**, 3220 (1995); **54**, 5515 (1996).

[19] P. Mathews and V. Ravindran, Int. J. Mod. Phys. A **11**, 2783 (1996).

[20] M. Glück, E. Reya, and C. Sieg, Phys. Lett. B **503**, 285 (2001).

[21] M. Glück, E. Reya, and C. Sieg, Eur. Phys. J. C **20**, 271 (2001).

[22] M. Fontannaz, Eur. Phys. J. C **38**, 297 (2004).

[23] P. Aurenche, M. Fontannaz, and J. P. Guillet, Z. Phys. C **64**, 621 (1994).

[24] P. Aurenche, M. Fontannaz, and J. P. Guillet, Eur. Phys. J. C **44**, 395 (2005).

[25] M. Glück, E. Reya, and I. Schienbein, Phys. Rev. D **60**, 054019 (1999); **62**, 019902 (2000); **63**, 074008 (2001).

[26] F. Cornet, P. Jankowski, M. Krawczyk, and A. Lorca, Phys. Rev. D **68**, 014010 (2003).

[27] F. Cornet, P. Jankowski, and M. Krawczyk, Phys. Rev. D **70**, 093004 (2004).

[28] T. Ueda, K. Sasaki, and T. Uematsu, Phys. Rev. D **75**, 114009 (2007).

[29] Y. Kitadono, K. Sasaki, T. Ueda, and T. Uematsu, Prog. Theor. Phys. **121**, 495 (2009).

[30] Y. Kitadono, K. Sasaki, T. Ueda, and T. Uematsu, Phys. Rev. D **81**, 074029 (2010).

[31] Y. Kitadono, Phys. Lett. B **702**, 135 (2011).

[32] Y. Yoshida, Prog. Theor. Phys. **123**, 79 (2010).

[33] K. Sasaki, Phys. Rev. D **22**, 2143 (1980).

[34] K. Sasaki, Prog. Theor. Phys. Suppl. **77**, 197 (1983).

[35] M. Stratmann and W. Vogelsang, Phys. Lett. B **386**, 370 (1996).

[36] K. Sasaki and T. Uematsu, Phys. Rev. D **59**, 114011 (1999).

[37] V. M. Budnev, V. L. Cheynyak, and I. F. Ginzburg, Nucl. Phys. **34**, 470 (1971).

[38] V. M. Budnev, I. F. Ginzburg, G. V. Meledin, and V. G. Serbo, Phys. Rep. **15**, 181 (1975).

[39] R. W. Brown and I. J. Muzinich, Phys. Rev. D **4**, 1496 (1971).

[40] C. E. Carlson and W. K. Tung, Phys. Rev. D **4**, 2873 (1971).

[41] K. Sasaki, J. Soffer, and T. Uematsu, Phys. Lett. B **522**, 22 (2001).

[42] K. Sasaki, J. Soffer, and T. Uematsu, Phys. Rev. D **66**, 034014 (2002).

[43] I. Schienbein, Ann. Phys. (N.Y.) **301**, 128 (2002).

[44] E. Reya, Phys. Lett. **124B**, 424 (1983).

[45] D. M. Scott and W. J. Stirling, Phys. Rev. D **29**, 157 (1984).

[46] M. Dress, M. Glück, and E. Reya, Phys. Rev. D **30**, 2316 (1984).

[47] D. A. Ross and L. J. Weston, Eur. Phys. J. C **18**, 593 (2001).

[48] S. D. Bass, Int. J. Mod. Phys. A **7**, 6039 (1992).

[49] A. V. Efermov and O. V. Teryaev, Phys. Lett. B **240**, 200 (1990).

[50] S. Narion, G. M. Shore, and G. Veneziano, Nucl. Phys. **B391**, 69 (1993); G. M. Shore and G. Veneziano, Mod. Phys. Lett. A **8**, 373 (1993); Nucl. Phys. **B381**, 23 (1992).

[51] A. Freund and L. M. Sehgal, Phys. Lett. B **341**, 90 (1994).

[52] S. D. Bass, S. J. Brodsky, and I. Schmidt, Phys. Lett. B **437**, 417 (1998).

[53] C. Bourrely, E. Leader, and J. Soffer, Phys. Rep. **59**, 95 (1980).

[54] J. Soffer, Phys. Rev. Lett. **74**, 1292 (1995).

[55] J. Soffer and O. V. Teryaev, Phys. Lett. B **419**, 400 (1998); **490**, 106 (2000).

[56] G. Bonneau, M. Gourdin, and F. Martin, Nucl. Phys. **B54**, 573 (1973); Z. Kunszt and V. M. Ter-Antonyan, Lett. Nuovo Cimento **4**, 940 (1972).

[57] C. Kounnas and D. A. Ross, Nucl. Phys. **B214**, 317 (1983).

[58] S. K. Jones and C. H. Llewellyn Smith, Nucl. Phys. **B217**, 145 (1983).

[59] Y. Kitadono, R. Sahara, T. Ueda, and T. Uematsu, Eur. Phys. J. C **70**, 999 (2010).